

The Role of Lithium Salts in the Conductivity and Phase Morphology of a Thermoplastic Polyurethane

J. D. van Heumen and J. R. Stevens*

Guelph–Waterloo Centre for Graduate Work in Chemistry, Guelph Campus,
University of Guelph, Guelph, Ontario, Canada N1G 2W1

Received July 26, 1994; Revised Manuscript Received March 23, 1995*

ABSTRACT: Fourier transform infrared spectroscopy (FT-IR), differential scanning calorimetry (DSC), and impedance spectroscopy (IS) were utilized to monitor changes in the morphology of a thermoplastic polyurethane (TPU) as a function of alkali-metal salt concentration. In this study, the alkali-metal salts of LiCF_3SO_3 and $\text{Li}(\text{CF}_3\text{SO}_2)_2\text{N}$ were observed to increase the overall bulk conductivity of a phase-segregated polyurethane comprising soft segments of poly(tetramethylene oxide) (PTMO) and hard segments of methylenebis(phenyl isocyanate) (MDI) and 1,4-butanediol (BDO). Significant changes occur in the FTIR spectrum of the TPU above the critical salt concentration (c_c) of 0.5 mmol/g of TPU, suggesting an interaction of the lithium cation within the hard segment and between the hard and soft phases. A loss in long-range ordering of the hard domain above c_c has also been observed by DSC. For temperatures around the hard segment T_g ($= 110^\circ\text{C}$) and above, IS revealed an increasing bulk conductivity as the salt concentration was increased. At lower temperatures a maximum in conductivity as a function of salt concentration occurs again at c_c . The results of this study would indicate that the characteristic phase-segregated morphology of the TPU has been altered as a result of the interaction of lithium cations within the polar hard domains and by the promotion of phase intermixing by the coupling of the hard and soft phases.

Introduction

Early work by Armand¹ and others² has prompted numerous investigations into the dissolution of alkali-metal salts in polyether polymers. The dissociation of alkali-metal salts is followed by the formation of transient cross-links between ether oxygens in the host polymer and alkali-metal cations; the anion is usually not solvated. Ionic transport occurs mainly through a coupling between the ions and polymer segmental motion; hence, polymers of high flexibility are essential in order to achieve the conductivities ($>10^{-5}$ S/cm) necessary to be useful in various ambient-temperature applications such as solid-state batteries,³ “smart” windows and other electrochromic devices,^{4,5} and fuel cells.⁶ In addition, these solid polymer electrolytes must also exhibit good dimensional stability and thus benefit from having elastomeric properties in their service temperature range.⁷ Early work using poly(ethylene oxide) (PEO) as the host polymer has shown that ionic conduction occurs mainly in the amorphous regions of the polymer.⁸ Considering the high tendency of PEO to crystallize at ambient temperature, many studies have attempted to increase the amorphous phase of the polymer by extensive structural modifications.^{9,10}

Thermoplastic polyurethanes (TPUs) are characterized by a two-phase morphology in which a soft phase containing either polyethers or polyesters is reinforced by condensation with a hard domain consisting of an aromatic diisocyanate extended with a short-chain diol.^{11,12} This phase-segregated morphology in which the hard and soft phases are thermodynamically incompatible is further enhanced by hydrogen bonding within the hard domain between the urethane $\text{C}=\text{O}$ and the $\text{N}-\text{H}$ moiety on an adjacent polymer chain segment. Complete phase segregation is never realized. Depending on the extent of phase intermixing, the boundary between the hard and soft domains is ill-defined. Consequently, a number of variables can affect the

elastomeric properties of the TPU. The most significant are the soft-segment molecular weight and the hard-segment concentration.¹³

Originally, Cooper and Tobolsky investigated the elastomeric properties of TPUs and from dynamic mechanical measurements suggested a phase-segregated morphology.¹⁴ More recently, numerous studies have attempted to elucidate the relationships between structure and properties within thermoplastic polyurethanes principally by the use of NMR,^{15,16} SAXS,^{17–19} DSC,^{20–23} and FTIR.^{24–28} DSC has been used extensively to examine the thermal characteristics of TPUs.^{20–23} In addition to the low-temperature T_g of the soft segment, it has been previously shown that polyurethanes of sufficient hard-segment concentration exhibit three endothermic transitions.²¹ These transitions include a low-temperature transition, t_1 (70 – 100°C), an intermediate transition, t_2 (120 – 170°C), and a high-temperature transition, t_3 (above 200°C). Assignments for these endothermic transitions are generally accepted as involving short-range ordering in the hard domain (t_1), long-range ordering (t_2), and microcrystallinity in the hard domain in TPUs of high hard-segment concentration (t_3).²³ Furthermore, annealing for extended periods at temperatures lower than t_3 results in a single endotherm, t_4 , approximately 20 – 50°C higher than that of the annealing temperature, replacing t_1 and t_2 . This has been attributed to improved long-range ordering within the hard domain at the expense of short-range ordering. There is also some indication that these multiple endotherms in TPUs have origins in discrete hard-segment crystal populations with different melting points.²² Seki²⁹ and McLennaghan^{30,31} have shown that the ionic salt doping of TPUs results not only in an increase in the soft-segment T_g but also in a loss of the higher temperature endothermic transitions.

Several investigations^{24–28} have examined the hydrogen-bonding characteristics of phase-segregated polyurethanes by FTIR in an attempt to discern these effects on the physical properties of TPUs. The regions of main interest are the $\text{N}-\text{H}$ region in which Lee²⁶ and Cole-

* Abstract published in *Advance ACS Abstracts*, May 1, 1995.

Table 1. T_g Temperatures for Lithium Salt Doped TPUs

[LiCF ₃ SO ₃] (mmol/g of TPU)	T_g (°C)	$\Delta T_g/\Delta c$ (°C/mmol/g of TPU)	[Li(CF ₃ SO ₂) ₂ N] (mmol/g of TPU)	T_g (°C)	$\Delta T_g/\Delta c$ (°C/mmol/g of TPU)
0.0	-44		0.0	-44	
0.15	-45		0.15	-34	70
0.30	-34	70	0.30	-32	40
0.67	-28	20	0.48	-30	30
1.5	-19	10	0.67	-17	40
2.0	-14	10			

Table 2. Melting Transition Temperatures and Heats of Melting for Lithium Salt Doped TPU^a

[LiCF ₃ SO ₃] (mmol/g of TPU)	t_1 (°C)	t_2 (°C)	t_4^b (°C)	ΔH_m (J/g)	[Li(CF ₃ SO ₂) ₂ N] (mmol/g of TPU)	t_1 (°C)	t_2 (°C)	t_4^b (°C)	ΔH_m (J/g)
0.0	108	150	156	2.6	0.0	108	150	156	2.6
0.15	105	134	159	1.3	0.15	64	134	156	2.1
0.30	108	126	155	0.47	0.30	108	132	154	1.2
0.67					0.48	78	135	155	0.1
1.5					0.67				
2.0									

^a When blanks occur in the table, no transitions were observed. ^b t_4 only observed after annealing at 140 °C for 45 min.

man²⁷ both observed that with increasing temperature the hydrogen-bonded N–H band at 3320 cm⁻¹ exhibits a reduced intensity. This was not accompanied with an increase in the free N–H band intensity at 3420 cm⁻¹. Previously it had been shown that the absorptivity coefficients are a strong function of the strength of hydrogen bonds as well as band frequency.^{27,28} As such, quantitative measurements from peak band areas in the N–H region may be erroneous if the absorptivity coefficients are not known with respect to hydrogen bond strength and band position. Of equal interest, the carbonyl region is less sensitive to absorptivity coefficient fluctuations; hence, band area determinations are an adequate reflection of functional group concentration. The carbonyl region is, however, sensitive to intrinsic ordering in the polymer. This region is defined by three carbonyl stretching vibrations: the “free” or non-hydrogen-bonded C=O (1730 cm⁻¹) and two stretching vibrations associated with disordered (1713 cm⁻¹) and ordered (1700 cm⁻¹) hydrogen-bonded C=O. The disordered H-bonded C=O corresponds to those hydrogen-bond interactions occurring within both amorphous and semicrystalline regions, while the ordered H-bonded C=O is characteristic of hydrogen bonds occurring within the crystalline hard domain.^{27,28} Watanabe et al.^{32,33} observed a hydrogen-bonded C=O band and non-hydrogen-bonded C=O band at respectively 1705 and 1730 cm⁻¹ in a poly(ether urethane urea) doped with LiClO₄. However, they did not report a change in the IR spectra with doping, suggesting a preferential solubility of the salt in the polyether phase. McLennaghan et al.^{30,31} examined a poly(ethylene oxide)-based TPU and observed a single carbonyl peak in the undoped spectra, which shifted to higher frequencies on the addition of NaI.

Although TPUs have been used previously as matrices for ionic conduction, it is unclear how the phase-segregated morphology of the TPU is affected by the incorporation of ionic salts. Our research investigates the effect that lithium trifluoromethanesulfonate (LiCF₃SO₃) and lithium trifluoromethanesulfonimide (Li(CF₃SO₂)₂N) has on the morphology and bulk impedance of a TPU of composition MDI/BDO/PTMO using FTIR, DSC, and IS.

Experimental Section

The TPU examined in this investigation (Estane 5714, BF Goodrich Co.) contains a PTMO soft segment and a hard segment of MDI and BDO and was used as received. The

solvents, dimethylformamide (DMF; Fisher) and tetrahydrofuran (THF; Fisher), were dried over 4-Å molecular sieves. The dopant salts, LiCF₃SO₃ (3 M) and Li(CF₃SO₂)₂N (3 M), were dried under reduced pressure (10⁻³ Torr) for 24 h at 110 °C.

Solutions of various lithium salt concentrations were prepared by dissolving both salt and TPU in DMF at 10 mass %. The solution was cast onto Teflon plates and the solvent slowly removed under a reduced pressure of 10⁻³ Torr for a minimum of 24 h at 80 °C. For FTIR analysis solutions containing 5 mass % of polymer and salt in THF were prepared. The solution was cast directly on NaCl plates, and the solvent was evaporated via a slow reduction of pressure at 110 °C for 24 h.

FTIR spectra were measured at ambient and elevated temperatures using a Nicolet system 4.4 instrument with a wavenumber resolution of 2 cm⁻¹. Band deconvolution of the resulting spectra was obtained by analysis with Grams 386 software (Galactic).³⁴ The maximum error associated with the deconvolution of the IR spectra is expected to be ±15%. In most cases the deconvolution was conducted several times to examine alternate deconvolutions for the same band envelope. Where bands are well-resolved the approximate error in calculating the band intensity is less than 10%.

DSC measurements were made over the temperature range -100 to +200 °C using a DuPont 2910 DSC instrument at a heating rate of 10 °C/min. The annealing experiments were conducted in the DSC at 140 °C for 45 min prior to commencing the temperature sweep. Impedance measurements were performed using thin films prepared by solvent evaporation with a diameter of 17 mm and an approximate thickness of 0.15 mm. Actual thickness measurements were conducted in the impedance cell by a micrometer device mounted as part of the cell construction. The ionic conductivities of the TPU, sandwiched between two stainless steel electrodes, were measured using a Hewlett-Packard 4192A computer interfaced for remote data collection.

Results and Discussion

DSC. DSC was utilized to examine the effect of LiCF₃SO₃ and Li(CF₃SO₂)₂N on the morphologically based thermal transitions of the TPU as well as the polyether soft segment T_g . Table 1 indicates an increase in the T_g of the PTMO soft segment as a function of salt concentration. Those lithium salts investigated raise the soft-segment glass transition temperature in a similar manner. This is consistent with other investigations of LiClO₄-doped TPUs containing either PEO^{30,31} or PPO^{32,33} as the soft segment. This is also well-known for polyether complexes with LiCF₃SO₃,³⁵ where an increase in T_g with salt concentration is observed. This indicates that the solvation of the lithium cation by the

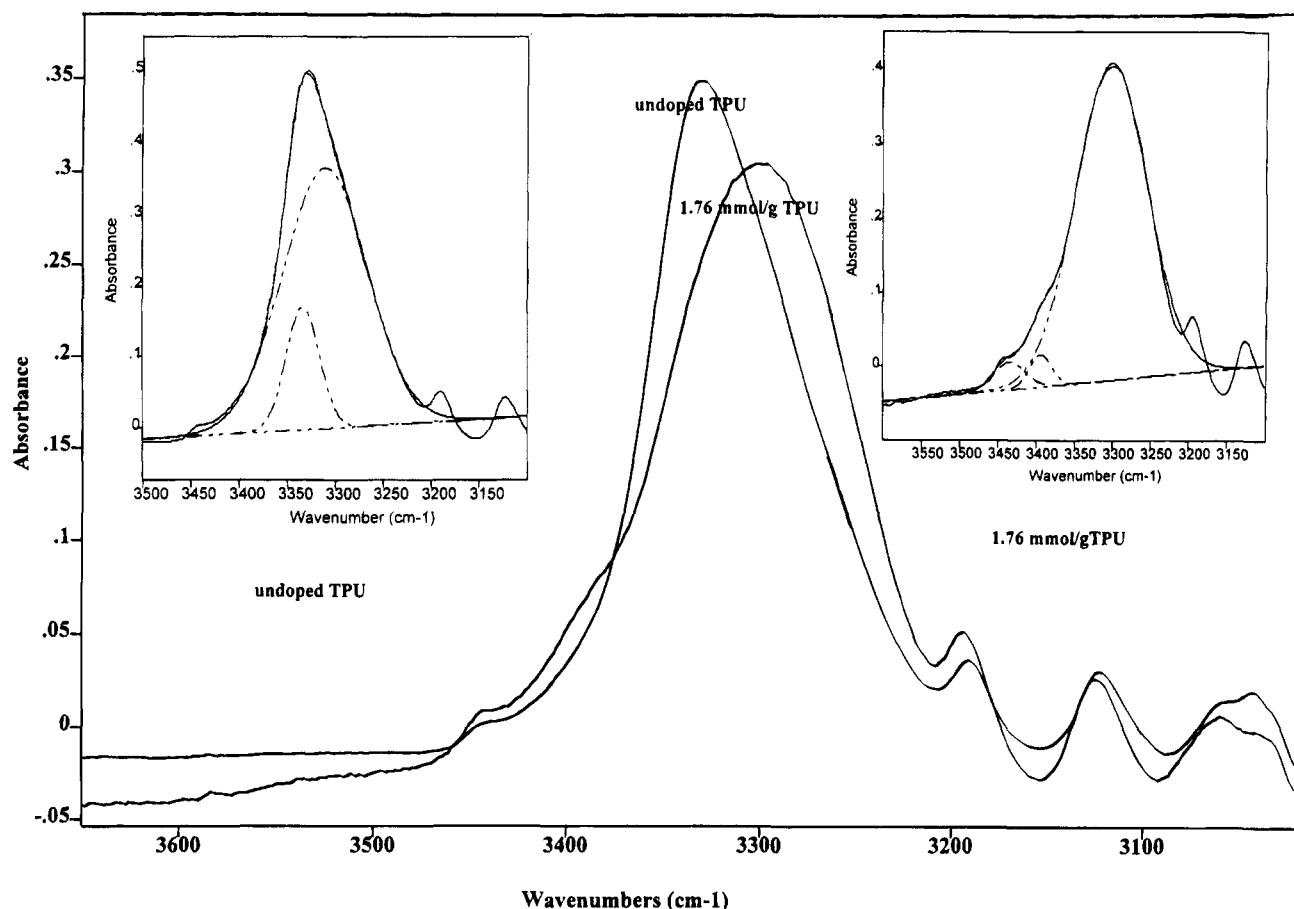


Figure 1. Relative IR absorbance in the N-H stretch region versus frequency in wavenumbers (cm^{-1}) for the undoped TPU and a TPU doped with 1.76 mmol of $\text{LiCF}_3\text{SO}_3/\text{g}$ of TPU.

PTMO soft segment partially arrests the local motion of the polymer segments through the formation of transient cross-links, resulting in an increase in the soft-segment T_g . By normalizing the T_g data with respect to concentration, $\Delta T_g/\Delta c$ was calculated at each measurement, and it is found that a linear increase in T_g is not observed with increasing salt concentration. As the salt concentration increases, $\Delta T_g/\Delta c$ generally decreases (Table 1). This does not appear unreasonable because of the plasticizing effect created by the formation of charge neutral contact ion pairs with increasing salt concentration.^{39,40} The neutral contact ion pairs lack the ability to form ionic cross-links; hence, further T_g increases are not observed. As stated earlier, endothermic transitions of a morphological origin in the hard domain can be examined by DSC. It has been observed that after annealing the TPU at 140 °C for 45 min t_1 and t_2 coalesce into a single transition at t_4 (≈ 155 °C); see Table 2. This new transition corresponds to the enhancement of long-range order. For this new morphology there is an incremental loss in the heat of melting, ΔH_m , at t_4 with increasing salt concentration, as seen in Table 2 where ΔH_m for the undoped TPU is 2.6 J/g at $t_4 = 156$ °C. This implies a reduction in the quantity of long-range-ordered regions in the TPU as the salt concentration is increased. The endotherm is no longer observed above 0.5 mmol/g of TPU (c_c). As t_4 is assigned to the long-range ordering within the hard domain, it can be inferred from observations that all lithium salts under investigation interact with the polar hard domain to eliminate any long-range ordering; a new morphology is created.

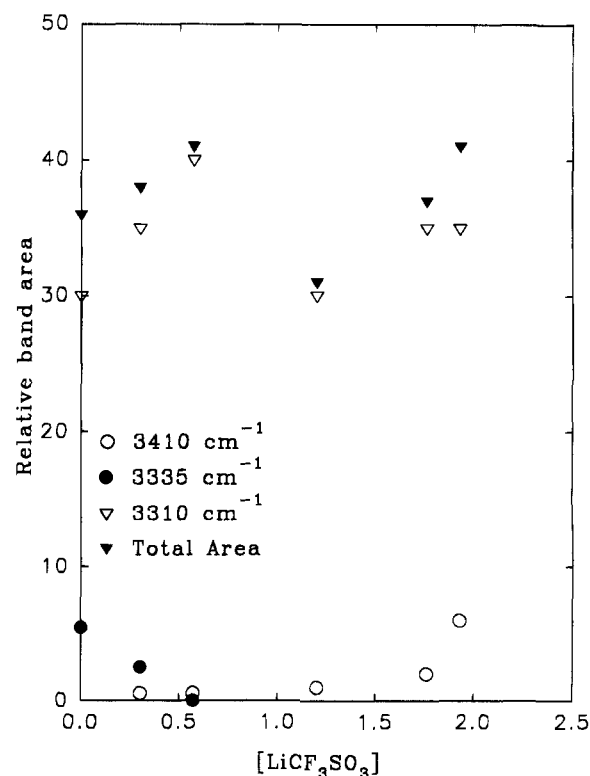


Figure 2. Relative band area of three modes in the N-H region vs LiCF_3SO_3 concentration: (○) Li-N-H, (●) overtone, (▽) H-bonded N-H.

FT-IR. In this work, FTIR has been utilized at both ambient and elevated temperatures to study the effects

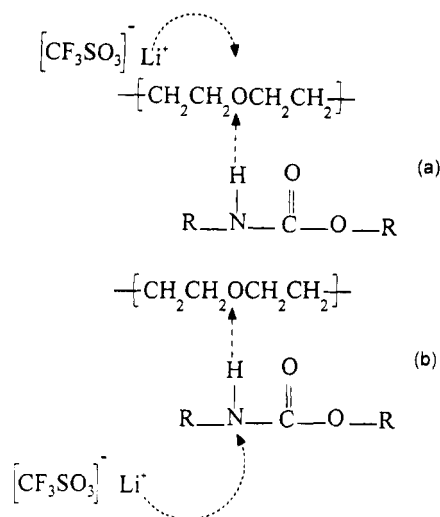


Figure 3. Schematics for the lithium cation-urethane moiety proposed as responsible for (a) the shift to lower frequency of the H-bonded N-H band and (b) the new feature at 3410 cm^{-1} .

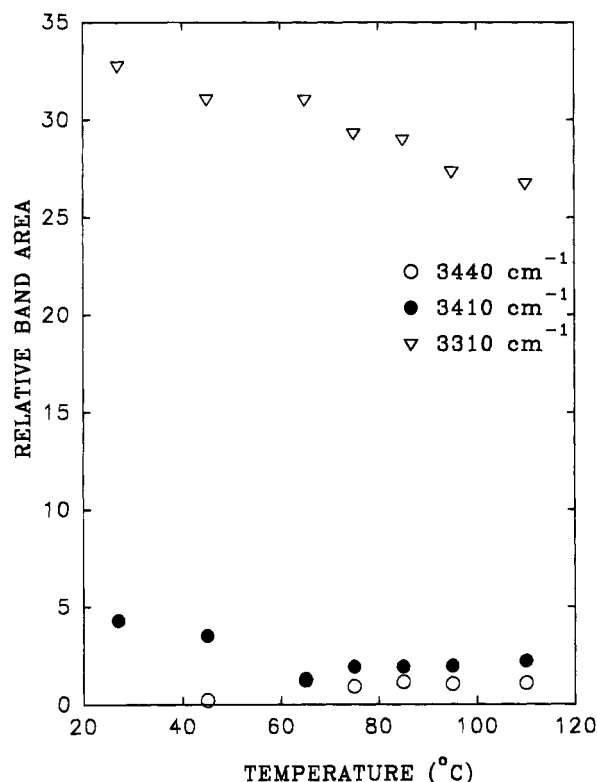


Figure 4. Relative band area versus temperature of the three modes in the N-H region: (○) Li-N-H, (●) overtone, (▽) H-bonded N-H.

of alkali-metal salt type and concentration on the phase morphology of the TPU. Four IR regions have been examined: (1) $3600\text{--}3100\text{ cm}^{-1}$, which includes the hydrogen-bonded N-H stretching mode and the free N-H stretch; (2) $1750\text{--}1650\text{ cm}^{-1}$, which includes the carbonyl symmetric stretch vibration or amide I band; (3) $1150\text{--}1000\text{ cm}^{-1}$, which includes the C-O-C stretch for the PTMO phase and the C(O)-O-C stretch of the hard phase; and (4) $1350\text{--}1150\text{ cm}^{-1}$, which includes the bending and stretching modes of the N-H and C-N moieties and the $\nu(\text{SO}_3)_a$ of CF_3SO_3^- . The carbonyl symmetric stretch is observed as a disordered and ordered hydrogen-bonded species at 1713 and 1700 cm^{-1} and as a free carbonyl at 1730 cm^{-1} . By examining the $\nu(\text{SO}_3)_a$ of CF_3SO_3^- , which is also present in this region,

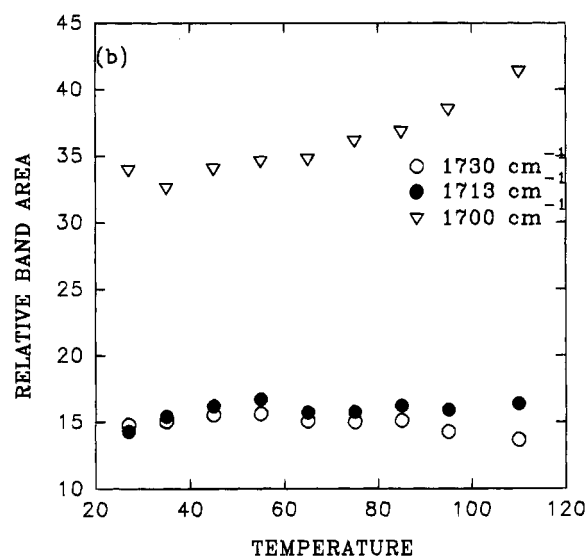
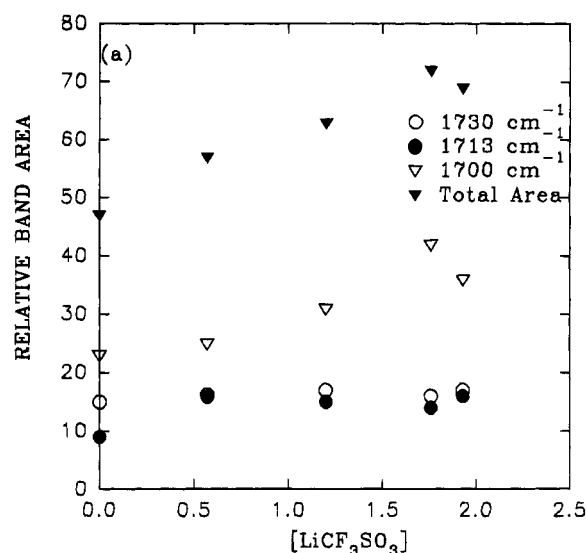


Figure 5. Relative IR band area versus salt concentration (a) and temperature (b) of the carbonyl region for a TPU doped with 2.0 mmol/g of TPU.

additional information is obtained regarding the formation of both free (CF_3SO_3^-) and contact ion pairs ($\text{Li}^+\text{CF}_3\text{SO}_3^-$). Additional information about contact ion pair formation can also be obtained from the $1350\text{--}1150\text{ cm}^{-1}$ region.

$3600\text{--}3100\text{ cm}^{-1}$. The N-H region is defined by at least two modes in a TPU.²⁷ The first, at 3440 cm^{-1} , is assigned to the free N-H stretching vibration, while the second, at 3310 cm^{-1} , is assigned to the hydrogen-bonded N-H stretch. In measurements of the IR spectra as a function of temperature the free N-H band could be resolved, while in the salt-doped TPUs it was difficult to deconvolute the contribution due to the free N-H. Therefore, the plots of relative band area as a function of salt concentration do not reflect the contribution due to free N-H. The temperature-dependent studies do show the contribution of free N-H where it was possible to deconvolute the free N-H component from the total band envelope. Shown previously by both Lee²⁶ and Coleman,²⁷ the free N-H band at 3440 cm^{-1} appears as a low-intensity shoulder on the measured 3310 cm^{-1} H-bonded N-H band and does not change

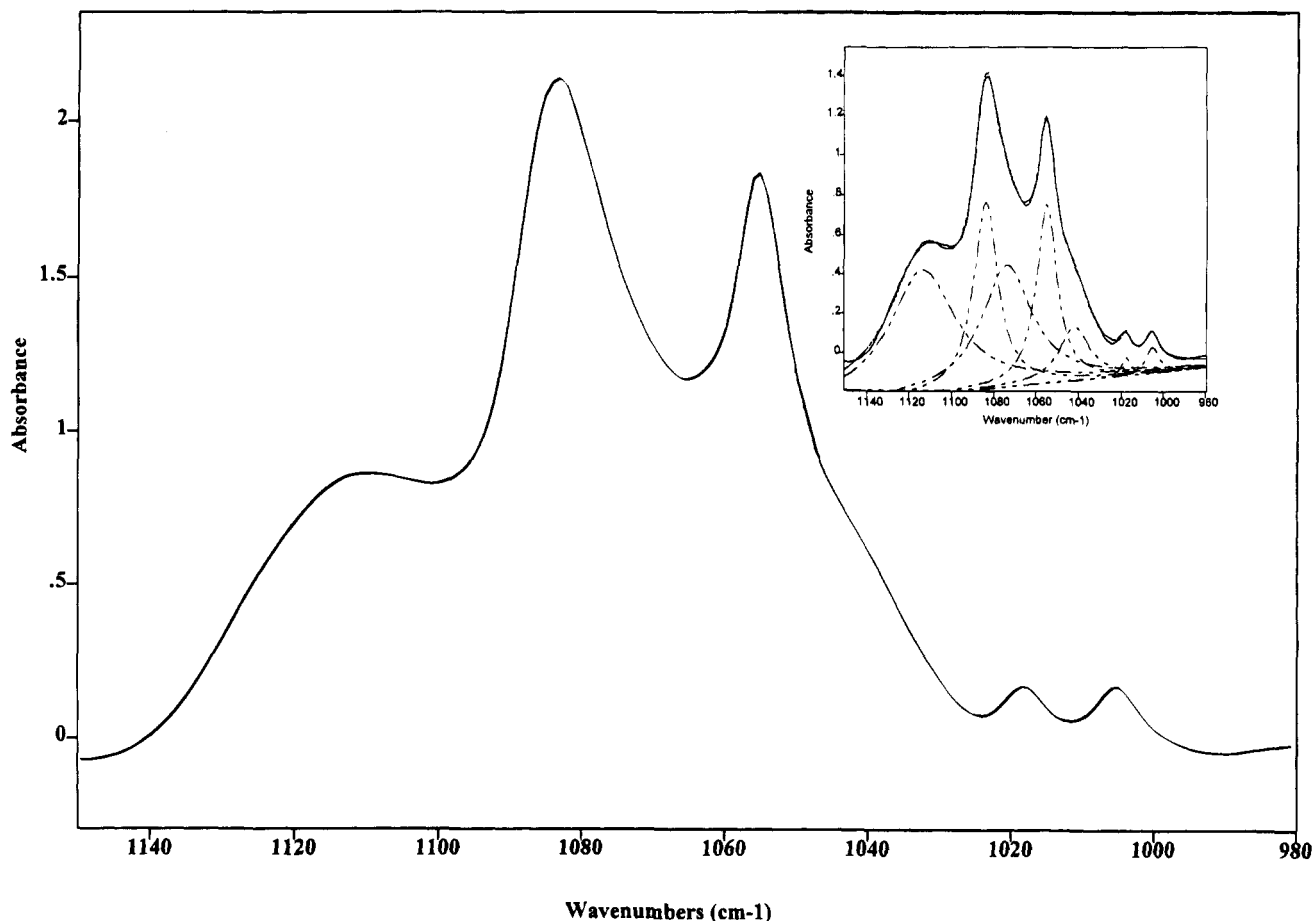


Figure 6. IR spectra and deconvolution of a TPU doped with 1.76 mmol/g of TPU in the 1150–980 cm^{-1} region.

markedly in intensity between 25 and 110 $^{\circ}\text{C}$. We have attempted to resolve it from the overall band envelope in order to gather more information about the effect of salt concentration on both the free and H-bonded modes of the N–H stretch.

In the undoped TPU, as seen in Figure 1, the skewed band envelope contains the free N–H mode as a low-intensity shoulder at 3440 cm^{-1} as well as an unassigned feature at 3335 cm^{-1} which could be assigned as the overtone to the fundamental in the carbonyl region.²⁷ Furthermore, the H-bonded N–H stretch is observed at 3310 cm^{-1} . At c_c , the 3335 cm^{-1} band is no longer observed and a new band emerges at 3410 cm^{-1} . Figure 1 illustrates the presence of this new band through the deconvolution of the TPU doped with 1.76 mmol/g of TPU. The new band reaches its highest level at 2.00 mmol/g of TPU as shown in Figure 2. All band areas were normalized to the CH_2 stretch of the PTMO soft segment. As well, the total band area was observed to be relatively constant over the salt concentration range investigated as seen in Figure 2. Above c_c , the H-bonded N–H band is not observed to change significantly with concentration, but a shift in band position was observed. The H-bonded N–H band was shifted from 3310 cm^{-1} , in the undoped TPU, to 3300 cm^{-1} at the highest salt concentration. Since band position is a function of the strength of the H-bonded N–H band, then the shift to lower frequency with an increase in salt concentration indicates a decrease in the bond strength of the N–H bond. This is likely due to the inductive effect of coordination of the Li^+ cation with the hydrogen-bonded species through the electron-rich oxygens as seen in Figure 3a. The free N–H shoulder

at 3440 cm^{-1} was observed to be relatively unaffected by salt doping and temperature. The new band at 3410 cm^{-1} is increasing in band area, which would suggest that ionic coordination occurs not only between the electron-rich oxygens in the TPU and Li^+ , as shown by DSC, but also between the electron-rich nitrogen of the urethane hard segment and the Li^+ . This type of coordination is not new. In an investigation of metal halide doping of Nylon 6, Dunn et al.³⁷ observed a new band emerging above 3400 cm^{-1} after treatment with LiCl . They assigned these spectral modifications to the formation of a nitrogen atom–metal ion coordinate bond. Recently, Lu and Weiss³⁸ investigated ionomer blends of manganese sulfonated polystyrene and Nylon 6 and also observed an additional absorption at 3520 cm^{-1} . The authors assigned the 3520 cm^{-1} mode to the delocalization of the lone pair electrons on the nitrogen as a result of coordination with the Mn^{2+} cation. Based on this information, the new band is assumed to be due to the interaction between and the Li^+ cation and the lone pair of electrons on the nitrogen atom, causing the N–H bond length to be reduced as seen in Figure 3b. Consequently, the vibrational energy of the bond will be increased and the IR position will be shifted to a higher frequency. This further indicates that the Li^+ cation is found in at least two distinct environments within the TPU matrix.

To further investigate the origins of the new band at 3410 cm^{-1} , temperature-dependent IR was conducted as shown in Figure 4. At the highest salt concentration there is a slow decrease in the relative band area for the 3410 cm^{-1} vibration with increasing temperature, as would be expected for a system containing transient

cross-links. The loss in band intensity is likely due to the decreased number of transient cross-links formed between the electron-donating nitrogen and the Li^+ cation. As well, the H-bonded N-H (3300 cm^{-1}) band area is decreasing in band area with increasing temperature, which is also a common occurrence for undoped TPUs.^{26,27} This band was also observed to shift from 3300 cm^{-1} at room temperature to 3317 cm^{-1} at 110°C . The shift of the band position to higher frequency at elevated temperatures is in contrast to the shift to lower frequency of the band position with increasing salt concentration. This indicates that the transient ionic cross-links formed within the polymer are temperature labile. Furthermore, to confirm that no degradation has occurred to the polymer matrix as a result of exposure to high temperature, measurements of the IR spectra were taken after the IR cell was cooled to room temperature; within experimental error the original spectral features were recovered.

1750–1650 cm^{-1} . Figure 5 illustrates the effect of increase in salt concentration and temperature on the three characteristic modes of the carbonyl region and the total band area. The free carbonyl stretch at 1730 cm^{-1} is unaffected by either salt concentration or temperature, while the ordered H-bonded carbonyl stretch at 1700 cm^{-1} is increasing in band area with an increase in salt concentration and temperature. The disordered H-bonded stretch at 1713 cm^{-1} increases in band area with an increase in salt concentration to a plateau level at c_c ; there is no temperature effect for this band. The band positions of all three modes were unaffected by salt doping. The fact that the carbonyl region is affected by the introduction of LiCF_3SO_3 suggests a further coordination between the carbonyl oxygen and the Li^+ of both the ordered and disordered phases. This is further observed by noting the increase in the total band area with increasing salt concentration. Given that the spectra have been normalized to a constant concentration of polymer, an increase in the total band area can only be accounted for by a change in the absorptivity coefficient with increasing salt concentration. For simple TPUs of alternating short-chain diol and diisocyanate only the ordered and disordered H-bonded C=O stretch vibrations have been observed to decrease in intensity with increased temperature.²⁷ This is contrary to the present observation for undoped TPUs where either no temperature effect is observed (disordered H-bonded carbonyl) or an increase in intensity with an increase in temperature is observed (ordered H-bonded carbonyl). It has already been noted that an increase in temperature causes a loss in the H-bonded N-H species. Thus, with increasing temperature it may be possible for the Li^+ cation dopant to penetrate the otherwise inaccessible ordering in the hard-segment domain, resulting in the coordination of the hard-segment C=O and the Li^+ .

1150–1000 cm^{-1} . The third region of interest, the ether oxygen region, consists of two major modes: the C–O–C stretch at 1115 cm^{-1} of the PTMO phase and the C(O)–O–C stretch of the hard-segment moiety at 1080 cm^{-1} in the undoped TPU. As salt is introduced into the polymer matrix the C(O)–O–C stretch at 1080 cm^{-1} is shifted to 1075 cm^{-1} , indicative of an inductive loss in electron density in the C–O–C bond of the hard segment as a result of coordination between the Li^+ and the carbonyl oxygen. The C–O–C stretch of the soft segment is unaffected. At c_c two additional bands emerge at 1085 and 1055 cm^{-1} (see Figure 6). Both of

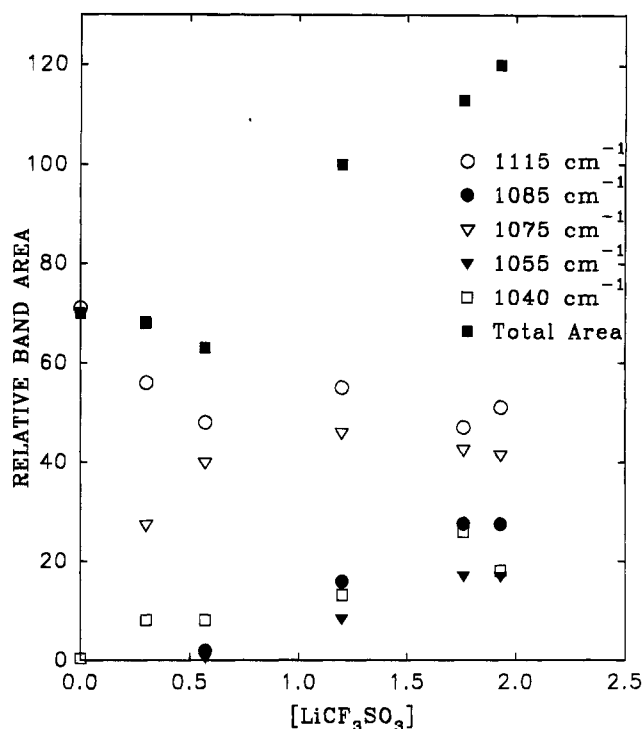


Figure 7. Relative IR band area as a function of salt concentration for the $1150\text{--}1000\text{ cm}^{-1}$ region.

these bands, increase in intensity with salt concentration above c_c , indicating a salt effect. The band intensity of the C–O–C (1115 cm^{-1}) decreases with increasing salt concentration; this is coupled with an increase in the band intensity of the 1085 cm^{-1} band (see Figure 7). The relative band intensity of the C(O)–O–C stretch increases and then decreases with increasing salt concentration, indicating the different coordination possibilities of the Li^+ cation, i.e., with C–O–C and C=O. Thus, it is postulated that these bands are the Li^+ complex formed with the ether oxygens of the PTMO phase (1085 cm^{-1}) and the carbamate oxygen of the hard segment (1055 cm^{-1}). This also suggests that the alkali-metal dopant is present in the hard domain, confirming the loss in long-range ordering of the hard segment also observed above c_c by DSC. Furthermore, the $\nu(\text{SO}_3)_s$ of the triflate anion is visible at 1040 cm^{-1} and increases in band area with increasing salt concentration. Many investigations have indicated the formation of contact ion pairs with both increasing salt concentration and increasing temperature.^{36,39,40} Although the higher frequency band (1040 cm^{-1}) assigned to contact ion pair formation ($\text{Li}^+\text{CF}_3\text{SO}_3^-$) was observed, the low frequency (1032 cm^{-1}) associated with the free CF_3SO_3^- was not. The free CF_3SO_3^- may be present but is difficult to resolve under the broad C–O–C band envelope. Furthermore, the total band area (Figure 7) sharply rises above the c_c which cannot be accounted for by changes in absorptivity but are more likely due to an increase in the concentration of ionic species having IR active bands in this region.

The temperature-dependent IR revealed that these complexes are surprisingly temperature insensitive. The entire C–O–C region remained unchanged with respect to band position and area with increasing temperature. This suggests that the addition of salt results in the formation of a complex which tends to stabilize the entire polymer toward temperature, more so than the undoped TPU.

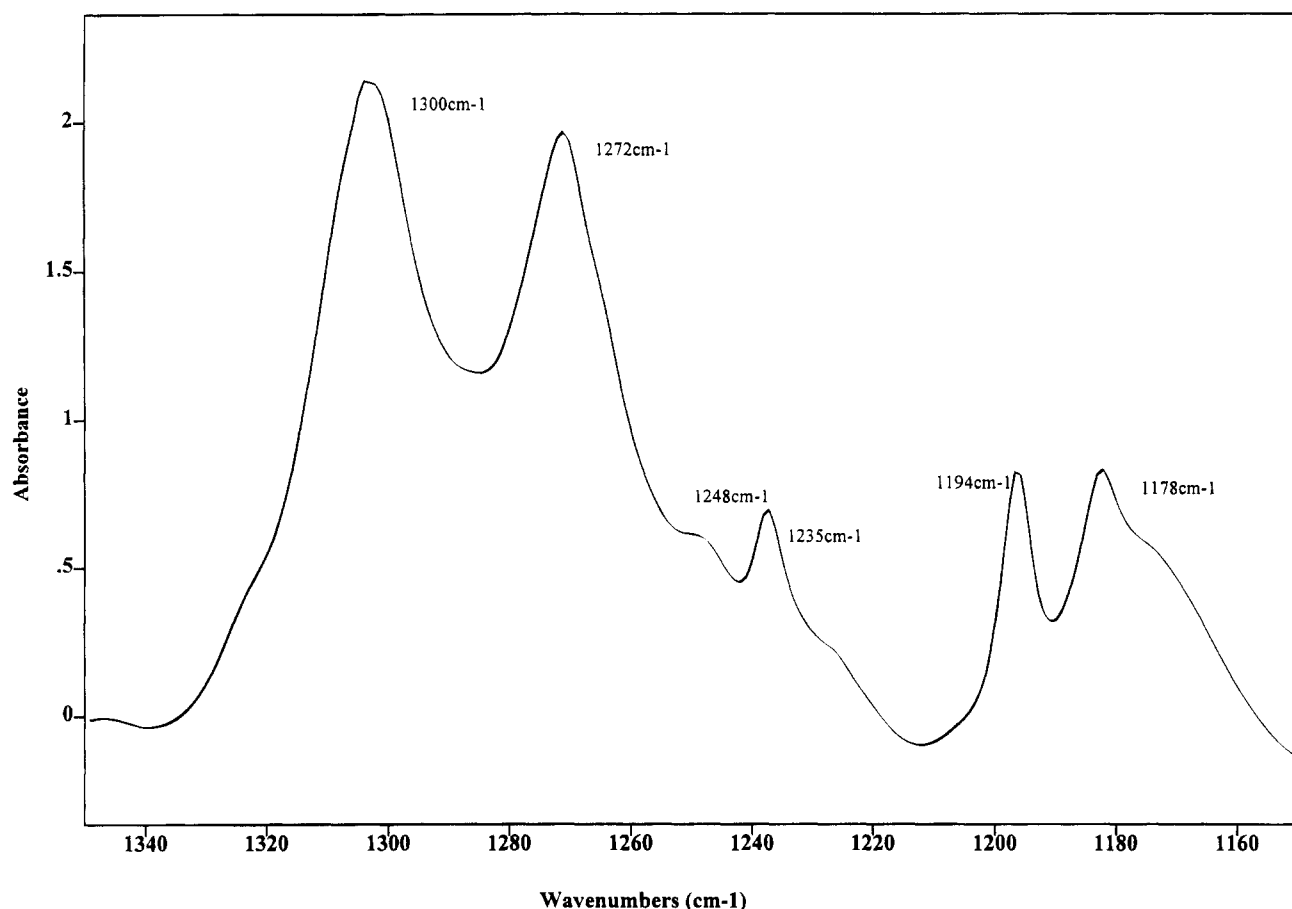


Figure 8. Subtracted IR spectra of LiCF_3SO_3 -doped TPU (2.00 mmol/g of TPU) from the undoped TPU in the region of 1350–1150 cm^{-1} .

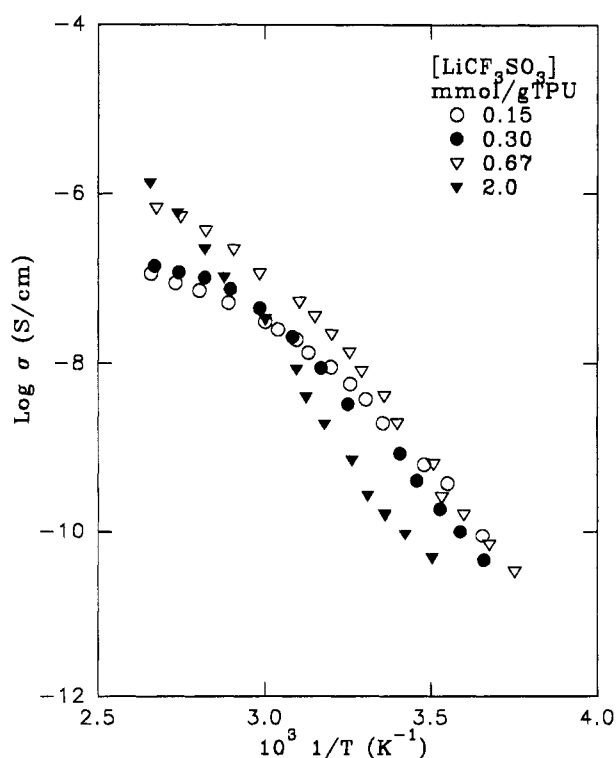


Figure 9. Ionic conductivity for the LiCF_3SO_3 -doped TPU plotted versus inverse temperature.

1350–1150 cm^{-1} . To further investigate the effect of salt doping on the IR of the PTMO-based TPU, the IR region of 1150–1350 cm^{-1} was also examined.

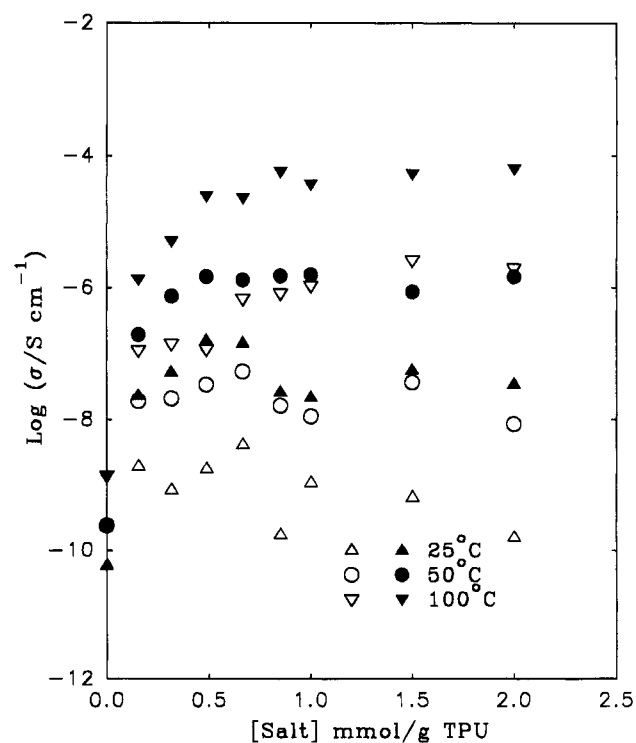


Figure 10. Conductivity isotherms at 25, 50, and 100 $^{\circ}\text{C}$ plotted versus salt concentration for LiCF_3SO_3 (open symbols) and $\text{Li}(\text{CF}_3\text{SO}_2)_2\text{N}$ (filled symbols) in TPU.

Figure 8 illustrates the IR region which contains the $\nu(\text{SO}_3)_a$ of the triflate anion. Again, above c_c of 0.5 mmol/g of TPU several new bands emerge in this region.

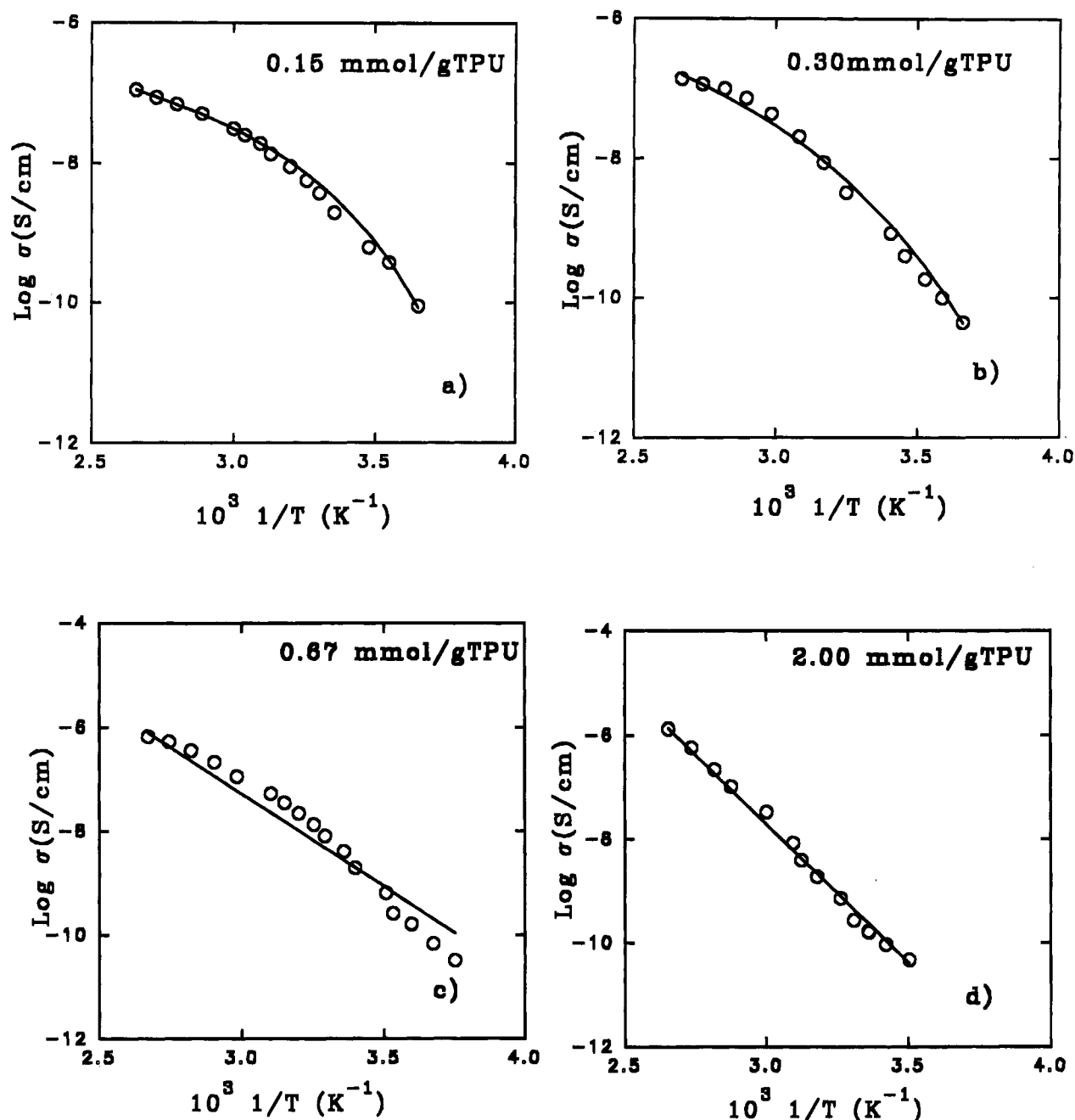


Figure 11. Conductivity data fit to VTF or Arrhenius phenomenological temperature relationships for LiCF_3SO_3 -doped TPU: (a) 0.15 mmol/g of TPU, (b) 0.30 mmol/g of TPU, (c) 0.67 mmol/g of TPU, (d) 2.00 mmol/g of TPU. VTF or Arrhenius fit (solid line): data points (\circ).

Previously it has been shown that when LiCF_3SO_3 is fully dissociated a single band at 1272 cm^{-1} is observed,³⁹ but in systems where contact ion pair formation is possible, the degeneracy of the band at 1272 cm^{-1} is removed and bands at 1300 and 1255 cm^{-1} are observed. In the LiCF_3SO_3 -doped TPU, two strong modes at 1300 and 1272 cm^{-1} have been observed, while a smaller shoulder on the low-frequency side of the 1272 cm^{-1} band has also been found at 1248 cm^{-1} , possibly corresponding to the 1255 cm^{-1} degenerate band. The strong 1300 cm^{-1} degenerate mode clearly does not correspond to an equally strong band at 1255 cm^{-1} in the doped TPU. Although Bernson et al. showed these bands to have a significant concentration dependence and a minimal temperature dependence,³⁹ it is unclear why the degenerate band at 1255 cm^{-1} is of such low band intensity while the degenerate band at 1300 cm^{-1} contributes significantly to the overall band area. Ad-

ditional bands at 1235 , 1224 , 1194 , and 1178 cm^{-1} also emerge above c_c . The $\nu(\text{CF}_3)_s$ is found at 1224 cm^{-1} , while the $\nu(\text{CF}_3)_a$ bands for both contact ion pairs and free triflate ions are observed at 1194 and 1178 cm^{-1} , respectively. These observations are different from those observed for $\text{LiCF}_3\text{SO}_3/\text{PPO}$ systems,³⁹ where bands with contact ion pairs (1299 and 1255 cm^{-1}) were observed with a hint of a band at 1272 cm^{-1} (free ions). This information would suggest that, even though the $\nu(\text{SO}_3)_s$ band (1032 cm^{-1}) associated with the solvated anion was not observed, there appear to be free anions present in the system.

Work is in progress to study this TPU system using FT-Raman. Initial results indicate support for the FTIR observations and will be reported.⁴¹

Impedance Analysis. There seems to have been little prior interest in TPUs as polymer electrolytes. Seki et al. doped TPUs of various hard-segment concentra-

tions and a MDI/BDO/PTMO composition with LiClO_4 .²⁹ In addition to observing a significant rise in bulk conductivity with an increase in salt concentration, the authors also concluded that an increase in the hard-segment concentration served to lower the overall bulk conductivity. Watanabe et al.^{32,33} examined a thermoplastic poly(urethane urea) of composition MDI/ED/PPO having a hard-segment concentration of 29%. The authors observed a decrease in conductivity with an increase in the concentration of LiClO_4 at 40 °C, while at 100 °C an increase in conductivity with increasing dopant concentration was found. As well, McLennaghan et al.^{30,31} have examined the effect of LiCF_3SO_3 and LiClO_4 on the conductivity and morphology of TPUs with various hard segment, MDI/BDO, concentrations and a soft segment of PEO. In addition to observing specific interactions between the hard phase and the lithium salt dopant, these authors observed a maximum conductivity for all isotherms shown.

Figure 9 illustrates the temperature dependence of ionic conductivity for LiCF_3SO_3 /TPU complexes. From this figure it is evident that increasing the concentration of the dopant does not significantly increase the bulk conductivity. The conductivity isotherms for both LiCF_3SO_3 - and $\text{Li}(\text{CF}_3\text{SO}_2)_2\text{N}$ -doped TPUs are illustrated in Figure 10. Similar to Watanabe et al.,³³ we observe a maximum conductivity at c_c at 25 and 50 °C, while at temperatures just below the T_g of the hard segment a maximum is not observed but the conductivity steadily increases. Contrary to that observed by McLennaghan et al.,³¹ a maximum conductivity is not observed as a function of concentration over the entire temperature range. These results may be explained by considering two factors. First, ion pair formation increases with alkali-metal salt concentration.⁴⁰ This limits the mobility of the charge carriers throughout the polymer matrix and is observable as a reduction in the bulk conductivity. Second, a considerable amount of salt is interacting or coordinating with the hard domain as has been observed by DSC and FTIR. The salt is unable to participate in the conductive process until the temperature region of the hard segment T_g (=110 °C) is reached. The observed rise in conductivity at 100 °C for both lithium salts is the result. The conductivity isotherms for $\text{Li}(\text{CF}_3\text{SO}_2)_2\text{N}$ (Figure 10) illustrate a significant rise in the bulk conductivity of the doped TPU over the entire temperature range. This may be due to limited coordination with the polymeric matrix as a result of the bulky structure of the anion.

The ionic conductivity data for the LiCF_3SO_3 -doped TPU as shown in Figure 9 was analyzed using the Vogel–Tammann–Fulcher (VTF) and Arrhenius phenomenological relationships shown below.

$$\sigma(T) = AT^{-1/2} \exp[-B/k_B(T - T_0)] \quad (\text{VTF}) \quad (1)$$

$$\sigma(T) = A \exp[-E/k_B T] \quad (\text{Arrhenius}) \quad (2)$$

The VTF form has mainly been used in describing the temperature dependence of ionic conductivity data. A is a constant, B is the pseudoactivation energy related to polymer segmental motion, k_B is the Boltzmann constant, and T_0 is a reference temperature usually associated with the ideal glass transition temperature at which free volume disappears or the temperature at which the configurational entropy becomes zero. In either case T_0 usually lies 35–50 K below the T_g . The application of the VTF form to ion transport in polymer

electrolytes requires a coupling of mobile charge carriers to the segmental motion of the polymer host. The Arrhenius form, in which E is the activation energy, is used when the ions are decoupled from the polymer host and activated hopping is required for ionic transport. Figure 11 illustrates fits for four concentrations, two above the critical concentration at which the morphology changes c_c (=0.50 mmol/g of TPU) and two below. It can be seen that below c_c the ions are predominantly coupled to the segmental motions of the host polymer since the VTF form provides the best fit. Above c_c , eq 2 is the best fit and activated hopping predominates. In the transition region (0.67 mmol/g of TPU) seen in Figure 11c it is interesting to note that the high-temperature values of the conductivity are fit with the VTF form and the low-temperature values are best fit with eq 2.

Conclusions

Doping TPUs by lithium salts, as observed by DSC and FTIR, is a method for altering the two-phase morphology of a thermoplastic polyurethane creating a new morphology which has improved temperature stability over the undoped TPU. Specific new coordinations between the lithium cation and the electron-rich components (nitrogen and oxygen) of the urethane moiety have been observed and aid in the creation of this new morphology. Furthermore, it can also be concluded that $\text{Li}(\text{CF}_3\text{SO}_2)_2\text{N}$ is a suitable salt for preparing a thermoplastic polyurethane polymer electrolyte in which conductivity and dimensional stability are required at high temperature (100 °C).

Acknowledgment. The work has been supported by Ontario Centre for Materials Research, Tremco Ltd., and BF Goodrich Co.

References and Notes

- Armand, M. B.; Chabagno, J. M.; Duclot, M. J. In *Fast Ion Transport in Solids*; Vashista, P., Mundy, J. N., Shenoy, G. K., Eds.; Elsevier–North-Holland: New York, 1979; p 131.
- Fenton, D. E.; Parker, D. E.; Wright, P. V. *Polymer* **1973**, *14*, 589.
- Gauthier, M.; Belanger, A.; Kapper, B.; Vassort, G.; Armand, M. In *Polymer Electrolytes Review 2*; MacCallum, J. R., Vincent, C. A., Eds.; Elsevier: London, 1989; p 285.
- Anderson, A. M.; Stevens, J. R.; Granqvist, C. G. In *Large Area Chromogenics—Materials and Devices for Transmittance Control Vol. IS4*; Lambert, C. M., Granqvist, C. G., Eds.; Institute Series; Opt. Eng. Press: Bellingham, USA, 1990; p 471.
- Hrai, Y.; Tapi, C. *Appl. Phys. Lett.* **1983**, *43*, 704.
- Przyluski, J.; Wieczorek, W. *Synth. Met.* **1991**, *45*, 323.
- Ratner, M. A.; Shriver, D. F. *Chem. Rev.* **1988**, *88*, 109.
- Harris, C. S.; Shriver, D. S.; Ratner, M. A. *Macromolecules* **1986**, *19*, 987.
- Gray, F. M. In *Solid Polymer Electrolytes—Fundamentals and Technological Applications*; VCH: Weinheim, Germany, 1991; Chapter 6.
- Cheradame, H.; Le Nest, J. F. In *Polymer Electrolyte Reviews I*; MacCallum, J. R., Vincent, C. A., Eds.; Elsevier: London, 1987; p 103.
- Gibson, P. E.; Vallance, M. A.; Cooper, S. L. In *Developments in Block Copolymers*; Applied Science Series; Elsevier: London, 1982.
- Van Bogart, J. V.; Gibson, P. E.; Cooper, S. L. *J. Polym. Sci., Polym. Phys. Ed.* **1983**, *21*, 65.
- Seefried, C. G., Jr.; Koleske, J. V.; Critchfield, F. E. *J. Appl. Polym. Sci.* **1975**, *19*, 2493.
- Cooper, S. L.; Tobolsky, A. V. *J. Appl. Polym. Sci.* **1967**, *11*, 1361.
- Dickinson, L. C.; Shi, J.; Chien, J. C. W. *Macromolecules* **1992**, *25*, 1224.
- Kricheldorf, H. R.; Hull, W. E. *Makromol. Chem.* **1981**, *182*, 1177.

- (17) Leung, L. M.; Koberstein, J. T. *J. Polym. Sci., Polym. Phys. Ed.* **1985**, *23*, 1883.
- (18) Miller, J. A.; Cooper, S. L. *J. Polym. Sci., Polym. Phys. Ed.* **1985**, *23*, 1065.
- (19) Li, Y.; Gao, T.; Chu, B. *Macromolecules* **1992**, *25*, 1737.
- (20) Seymour, R. W.; Cooper, S. L. *Macromolecules* **1973**, *6*, 48.
- (21) Hesketh, T. R.; Van Bogart, J. W. C.; Cooper, S. L. *Polym. Eng. Sci.* **1980**, *20*, 190.
- (22) Koberstein, J. T.; Galambos, A. F. *Macromolecules* **1992**, *25*, 5618.
- (23) Leung, L. M.; Koberstein, J. T. *Macromolecules* **1986**, *19*, 706.
- (24) Srichatrapimuk, V. W.; Cooper, S. L. *J. Macromol. Sci., Phys.* **1978**, *15*, 267.
- (25) Senich, S. A.; MacKnight, W. J. *Macromolecules* **1980**, *13*, 106.
- (26) Lee, H. S.; Wang, Y. K.; Hsu, S. L. *Macromolecules* **1987**, *20*, 2089.
- (27) Coleman, M. M.; Lee, K. H.; Skrovanek, D. J.; Painter, P. C. *Macromolecules* **1986**, *19*, 2149.
- (28) Coleman, M. M.; Skrovanek, D. J.; Howe, S. E.; Painter, P. C. *Macromolecules* **1985**, *18*, 299.
- (29) Seki, M.; Sato, K. *Macromol. Chem.* **1992**, *193*, 2971.
- (30) McLennaghan, A. W.; Pethrick, R. A. *Eur. Polym. J.* **1988**, *24*, 1063.
- (31) McLennaghan, A. W.; Hooper, A.; Pethrick, R. A. *Eur. Polym. J.* **1989**, *25*, 1297.
- (32) Watanabe, M.; Oohashi, S.; Sanui, K.; Ogata, N.; Kobayashi, T.; Ohtaki, Z. *Macromolecules* **1985**, *18*, 1945.
- (33) Watanabe, M.; Sanui, K.; Ogata, N. *Macromolecules* **1986**, *19*, 815.
- (34) Grams 386 is a commercially available product from Galactic Industries Corp. Marquardt's nonlinear least-squares fitting algorithm is used. Marquardt, D. W. *J. Soc. Int. Appl. Math.* **1963**, *11*, 431.
- (35) Albinsson, I.; Mellander, B.-E.; Stevens, J. R. *J. Chem. Phys.* **1992**, *96*, 681.
- (36) Bernson, A.; Lindgren, L. *Solid State Ionics* **1993**, *60*, 37.
- (37) Dunn, P.; Sansom, G. F. *J. Appl. Polym. Sci.* **1969**, *13*, 1657.
- (38) Lu, X.; Weiss, R. A. *Macromolecules* **1991**, *24*, 4381.
- (39) Kakihana, M.; Schantz, S.; Torell, L. M. *J. Chem. Phys.* **1990**, *92*, 6271.
- (40) Schantz, S.; Torell, L. M.; Stevens, J. R. *J. Chem. Phys.* **1991**, *94*, 6862.
- (41) Ferry, A.; Jacobsson, P.; van Heumen, J. D.; Stevens, J. R. Submitted to *Polymer*.

MA946210B